Journal of Cellular Biochemistry 85:798–808 (2002)

Chromatin of *Trypanosoma cruzi*: In Situ Analysis Revealed Its Unusual Structure and Nuclear Organization

Barbara Spadiliero,[1]* Claudio Nicolini,[2,3] Giancarlo Mascetti,[2] Diana Henríquez,[1] and Laura Vergani[2]

[1]Department of Cell Biology, Simón Bolívar University, Caracas 89 000, Venezuela
[2]Department of Biophysical Sciences and Technologies M & O, School of Medicine, University of Genova, Genova 16132, Italy
[3]ELBA Foundation, Via delle Testuggini Roma, Italy

Abstract Chromatin of *Trypanosoma cruzi* is known to be organized in classical nucleosomal filaments, but surprisingly, these filaments do not fold in visible chromosomes and the nuclear envelope is preserved during cell division. Our hypothesis about the role of chromatin structure in regulating gene expression and, more generally, cell functioning, pressed us to verify if chromatin organization is modulated during the parasite life-cycle. To this end, we analyzed in situ the fine structural organization of *T. cruzi* chromatin by means of an integrated biophysical approach, using differential scanning calorimetry and fluorescence microscopy. We observed that logarithmic forms exhibit a less condensed chromatin with respect to the stationary ones. Thermal analysis revealed that parasite chromatin is organized in three main levels of condensation, barring from the polynucleosomal filament till to superstructured fibers. Besides, the fluorescence images of nuclei showed a characteristic chromatin distribution, with defined domains localized near to the nuclear envelope. While in stationary parasites, these regions are highly condensed, in logarithmic forms they unfold by extending themselves toward the center of nucleus. These observations suggest that, in comparison with higher eukaryotes, in *T. cruzi* the nuclear envelope plays an unusual and pivotal role in interphase and in mitosis. J. Cell. Biochem. 85: 798–808, 2002.

Key words: *Trypanosoma cruzi*; parasite life-cycle; chromatin structure; nuclear architecture

Trypanosoma cruzi is a protozoan parasite, responsible for Chagas disease that afflicts 16–18 million people in South and Central America [Herwaldt, 1999]. This disease is of significant medical and economical importance. In fact, prophylactic treatments are available, but they are proving unsatisfactory due to high cost, side effects, and the increasing emergence of drug resistance.

During its life-cycle, *Trypanosoma cruzi* undergoes complex morphological and biochemical changes [Schmidt and Roberts, 1989; Sabaj et al., 1997; Belli, 2000] as it differentiates and adapts to variables environments. The life cycle of *T. cruzi* can be summarized as follows. When an insect infected with *T. cruzi* bites a mammalian host, it releases trypomastigotes in the feces or urine. Through the blood stream, trypomastigotes can infect neighboring cells; inside the cell trypomastigotes differentiate into amastigotes, some of which are capable of multiplying and redifferentiatiating into trypomastigotes. Newly transformed trypomastigotes leave the infected cell to initiate a new cycle in adjacent cells, or they can enter the circulation. In this way, they can propagate the infection throughout the body. When the hemotophagous reduviid insect feeds on blood of the infected animal, it initiates a cycle in the invertebrate host. In the midgut of the insect, trypomastigotes transform into epimastigotes,

Grant sponsor: University of Genova; Grant sponsor: European Community (INTAS Project); Grant number: 93-12446; Grant sponsor: Ministry of Education, University, and Research (to ELBA Foundation).

*Correspondence to: Barbara Spadiliero, DISTBIMO, Corso Europa 30, 16132 Genova, Italy.
E-mail: bspadi@usb.ve

Received 9 January 2002; Accepted 25 February 2002
DOI 10.1002/jcb.10183

which in the rectal glands differentiate again into trypomastigotes, which in turn are released and eliminated with the feces during a blood meal.

As a consequence of a complex life cycle, this parasite is forced to make rapid adaptations to different environments, which require dramatic changes on gene expression. These alterations can be accompanied by modifications of chromatin structure and nuclear organization. The hypothesis that chromatin structure can play a crucial role in the regulation of DNA transcriptional activity records an increasing consensus [Wolffe and Hayes, 1999; Wolffe and Matzke, 1999; Belli, 2000]. Moreover, it has been recently observed how nuclear localization of genes is critical for their expression, e.g., silent genes are often localized inside the interphase chromosomes, while active ones are observed in the periphery [Kurz et al., 1996; Zinc et al., 1998].

Chromatin of *T. cruzi* was described [Rubio et al., 1980; Astolfi et al., 1980] as organized in nucleosomal filaments typical of higher eukaryotes. Despite these similarities, mitosis is characterized by unusual features: chromatin fibers do not form visible chromosomes, a presence of a spindle pole was not observed, and the nuclear membrane persists during the process. The unusual behavior of *T. cruzi* chromatin has been partially explained by the biochemical differences between histones of *T. cruzi* and histones of higher eukaryotes [Toro and Galanti, 1990; Toro et al., 1993; reviewed by Hecker et al., 1994; Sabaj et al., 1997]. In the last years, different approaches have been employed to characterize in vitro the folding of chromatin fibers isolated from different forms of *T. cruzi* [Astolfi et al., 1980; Rubio et al., 1980; Hecker and Gander, 1985; Hecker et al., 1989; Schlimme et al., 1993; Spadiliero et al., 2002], but they encountered several problems due to chromatin aggregation and fragility, mainly at physiological salt conditions. For this reason, we choose to employ differential scanning calorimetry (DSC) that has proved to be very useful for studying chromatin structure because it does not require optically clear samples as it is instead necessary for spectroscopy studies [Nicolini et al., 1983; Touchette and Cole, 1985; Balbi et al., 1989]. As previously reported [Gavazzo et al., 1997; Vergani et al., 1998], the thermal denaturation profile of native eukaryotic nuclei can give information about the average condensation of the nuclear chromatin.

According to the approach followed in previous works of our group [Nicolini et al., 1997; Vergani et al., 1998; Vergani et al., 1999; Mascetti et al., 2001], the thermodynamic analysis performed on native nuclei can be integrated by the quantitative results obtained by high resolution fluorescence microscopy performed on intact cells stained with a DNA selective dye [Hiraoka et al., 1987; Mascetti et al., 1996]. This technique allows us to quantitatively analyze in situ the chromatin organization and the nuclear architecture through a deep analysis of the distribution of the fluorescent dye (DAPI in our case) used for labeling the DNA. Previous published works [Myc et al., 1992; Vergani et al., 1992; Nicolini et al., 1997] demonstrated that the integrated fluorescence intensity of an entire nucleus is directly dependent on the level of chromatin condensation, keeping constant the DNA content. After an appropriate mathematical processing of the acquired digital images, we can obtain a fine characterization of the organization and structural features of in situ chromatin [Mascetti et al., 1996, 2001].

Starting from previous works [Hecker et al., 1989; Spadiliero et al, 2002] on the structure of *T. cruzi* chromatin, which showed a reduced stability and an abnormal compaction pattern with respect to higher eukaryotes, we are interested in understanding, at a structural level, the peculiarity of *T. cruzi* chromatin and in correlating this information with data about the transcription regulation of the parasite. To this end, we studied the differences at the level of chromatin structure between two different forms of *T. cruzi*: epimastigotes in logarithmic and stationary phase of growth, respectively.

MATERIALS AND METHODS

Culture of *T. cruzi*

The proliferative forms of *T. cruzi*, originally isolated from a Venezuelan patient (EP), were grown at 27°C in LIT (liver infusion tryptose: 0.15 M NaCl; 5.36 mM KCl; 0.005 M Na_2HPO_4; 0.02 M glucose; 0.03 mM hemin; 1.5% bactotryptose; 0.5% yeast extract; 0.5% liver broth; 10% heat inactivated fetal calf serum). Cultures were maintained in exponential growth through periodic passages into fresh medium.

Epimastigotes are the replicative cellular forms of *T. cruzi*, which can be readily cultivated. For our experiments, the logarithmic-phase forms were collected at day 5 of culture, while the stationary-phase forms were collected at day 14 of culture.

Nuclei Isolation

Nuclei from fresh *T. cruzi* culture were prepared in the cold and in presence of protease inhibitors (0.5 mM tosyl-lysine chloromethyl ketone (TLCK), 2 mM phenyl-methyl-sulphonyl-fluoride (PMSF), 1 mM N-ethilmalemide; 0.5 tosyl-phenil chloromethyl ketone (TPCK)), according to Astolfi et al. [1980] with slight modifications. Parasites (about 1×109) were collected by low-speed centrifugation (500*g*, 10 min) and washed once with PBS (buffer saline phosphate, 0.2% KCl; 0.2% KH_2PO_4; 8% NaCl; 0.93% Na_2HPO_4 pH 7.0) and once in Buffer A (20 mM Tris-HCl pH 8.0; 1 mM $MgCl_2$; 250 mM sucrose; 0.01% spermidine; 0.005% spermine). Cells were then resuspended in 2 ml of Buffer B (20 mM Tris-HCl pH 8.0; 1 mM MgCl2; 5 mM KCl; 3 mM CaCl2; 1% NP-40; 0.01% spermidine; 0.005% spermine; 15 mM β-mercaptoethanol) and subsequentely lysed with 50 strokes with a Teflon dounce homogenizer. The lysate was centrifuged for 5 min at 500*g*; the recovered supernatant was centrifuged for 10 min at 2000*g*. The resulting pellet was first resuspended in 2 ml of Buffer B without NP-40 and then diluted with 6 ml of Buffer C (20 mM Tris-HCl pH 8.0; 1 mM $MgCl_2$; 5 mM KCl; 0.2 mM $CaCl_2$; 2 M sucrose; 0.1% spermidine; 0.005% spermine; 15 mM β-mercaptoethanol). The suspension was layered over 2 mL cushion of Buffer C and centrifuged at 120,000*g* for 60 min at 4°C in a Beckman SW 41.1 rotor.

Rat liver nuclei were obtained according to Burgoyne et al. [1970]. Isolation, washing, and assay were carried out in Buffer A (60 mM KCl, 15 mM NaCl, 0.5 mM spermidine, 0.15 mM spermine, 15 mM 2-mercaptoethanol, 15 mM tris-chloride, pH 7.4) with additions as indicated. Liver from an adult rat was rapidly homogenized in at least 7 ml/g of liver of Buffer A-0.34 mM sucrose, 2 mM EDTA, 0.5 mM EGTA. The homogenate was layered on a 0.33 volume of Buffer A-1.37 M sucrose, 1 mM EDTA (ethylen tiamine-tetra-acetic acid), 0.25 mM EGTA, and centrifuged for 15 min at 16,000*g*. The nuclear pellet was resuspended in 7 volumes of the same buffer and centrifuged for 4 min at 75,000*g*. The pellet was washed in Buffer A-0.34 M sucrose by centrifuging for 15 min at 16,000*g*.

DNase I Digestion

Nuclei from *T. cruzi* parasites were resuspended in digestion buffer (60 mM KCl; 15 mM; spermine; 0.5 mM spermidine; 15 mM Tris-HCl pH 7.4; 1.9 M sucrose; 0.1 mM Na_2EDTA) and digested with 0.06 U per 20 A260/ml of DNase I at 37°C for 30 min. Digestion was stopped by adding 20 μL of 0.1 M Na_2EDTA/ml, and the nuclear suspension was chilled on ice. The nuclei were centrifugated at 4,000*g* for 15 min. After washing with RSB (run on saline buffer: Tris-HCl 10 mM pH 7.4, NaCl 15 mM, $MgCl_2$ 1.5 mM), the nuclear pellet was centrifuged at 8,000*g* for 60 min at 4°C. The nuclear enriched pellet was utilized for DSC experiments.

Differential Scanning Calorimetry

Calorimetric experiments were run on a Perkin Elmer DSC-2 (Perkin Elmer Corporation, Norwalk, CT) interfaced with a computerized system that guarantees good reproducibility and sensitivity and great potential for signal acquisition, background subtraction, and data display. As previously described [Nicolini et al., 1988], measurements were performed in 100 μL stainless-steel capsules, in a temperature range between 310 and 410 K at a low scanning rate of 5 K/min, high sensitivity of 0.1 mcal/s, and high sample size (about 60 mg). At least three different measurements were acquired for each sample in order to check the accuracy and statistical significance of the experiments.

Deconvolution of the heat capacity profiles into Gaussian components was carried out by least square fitting of the acquired data after subtraction of the corresponding baseline. The baselines were obtained by a new thermal scanning of the denatured sample.

Calorimetric measurements were performed on native nuclei extracted from *T. cruzi* and rat liver as previously described in this section.

High Resolution Fluorescence Microscopy

Parasites from logarithmic and stationary phase of growth were washed in PBS and centrifuged at 500*g* for 10 min. Parasites were fixed overnight at 4°C in the fixation buffer (PBS $1 \times$, 0.75% formaldehyde, 2% glutaraldehyde, 2 mM $MgCl_2$, 2 mM EDTA). After fixation, parasites were washed three times in PBS and permebilized with 0.1% Triton X-100 in PBS $1 \times$ for 1 min

at room temperature. After washing, parasites were resuspended in 15 μM of 2′,6-diamidino-2-phenylindole (DAPI) for 20 min at room temperature. Excess of DAPI was eliminated washing with PBS; parasites were resuspended in PBS and observed.

For the acquisitions, we used a Zeiss Axioplan light microscope (Zeiss, Oberoken, FRG) modified for computer controlled stage, shutter, focus, and data acquisition [Mascetti et al., 1996] with a Zeiss Plan-Neofluar 100 ×NA = 1.3 oil immersion lens. The standard epifluorescence set-up for DAPI was employed. Digital pictures were obtained by an air-cooled (−50°C) scientific grade Charged Coupled Device (CCD) camera (ORCA II, Hamamatsu Photonics, Japan) with a dynamic range of 14 bits (grey levels from 0–16,383). The CCD camera exhibits excellent linearity within the range of utilization and low light sensitivity [Hiraoka et al., 1987]. The optical resolution element (pixel), at our level of magnification, corresponds with 67×67 nm^2 in the object plane. Shading correction and dark image subtraction have been applied to the acquired images in order to obtain a quantitative representation of fluorescence intensity. Such techniques are always applied when CCD cameras are used as imaging systems, in order to calibrate for non-uniformity of bi-dimensional illumination pattern and to take into account for CCD array non-homogeneous [Hiraoka et al., 1987].

For the optical sectioning, the nuclear images were acquired at different focal positions (0.1 μm intervals) along the z-axis in order to have from 64–128 slices within the sample. For each sample, the images of about 5–10 cells were acquired and processed using proper software for image analysis.

Digital Image Processing

Before the quantitative image analysis, each three-dimensional stack was deconvolved by the theoretical point spread function (PSF) in order to reduce the geometrical distortions introduced by optics along the optical axis. In order to increase the signal to noise ratio, a mathematical pre-processing was performed using a free software called OCTAVE (Department of Chemical Engineering, University of Wisconsin, WI). For the image processing of each three-dimensional stack, we used a tool called XCOSM (Biomedical Computer Laboratory, Washington University, WA). Mathematical corrections and deconvolution procedures were applied to each nuclear stack in order to visualize and analyze the internal features that are not directly visible in the original acquired stack.

Transmission Electron Microscopy Analysis of Thin Nuclear Sections

Nuclei were isolated from *T. cruzi* and rat liver, and they were prepared for thin-sectioning and electron microscopy according to Hecker and Gander [1985] with slight differences [Spadiliero et al., 2002]. Breaving, an enriched fraction of nuclei, was fixed in glutaraldehyde 2.5% in PBS 1 × at 4°C overnight. The fixed pellet was minced and fixed in osmium tetroxide 1%, 246 mosm/L in PBS 1 ×, 1 h at 4°C. After washing the sample carefully, it was dehydrated progressively with ethanol 50, 70, 80, 90, and 100% for 5 min at 4°C. Nuclei were washed first into propylene oxide:ethanol 1:1 followed by propylene oxide 100% for 15 min at 4°C each. The samples were imbibed in Polibet 812 resin and polymerized at 60°C for 48 h. The sections were obtained in a Porte–Blum equipped with a diamond knife. The sections of 60 nm were stained with uranyl acetate and lead citrate [Reynolds, 1963]. Thin sections were disposed over a carbon-coated grid of 200 nm covered with collodium and carbon film. The adsorption was allowed for 5 min at room temperature. The grids were examined in a Philips CM-10 transmission electron microscope at a 16,000–20,000 × [Spadiliero et al., 2002].

RESULTS

Structural Characterization of the Higher-Order Chromatin Structure by Differential Scanning Calorimetry

DSC analysis of nuclei purified from logarithmic and stationary forms of *T. cruzi* revealed significant differences of higher-order chromatin structure, strictly related with the phases of cell growth. In this analysis, the nuclear sample is subjected to a progressive heating, which induces different thermal transitions associated with the melting of specific molecular components. Therefore, a thermogram consists of a series of heat absorption peaks, each of them corresponding to the unfolding of an energetically-distinguishable molecular domain.

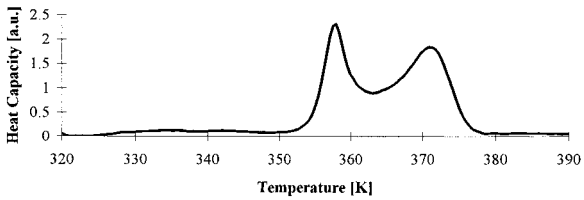

Fig. 1. Thermal denaturation profile of nuclei isolated from rat hepatocytes. Rat hepatocytes represent the control of DSC experiments on *T. cruzi*. DSC acquisition was performed as described in Materials and Methods. We can identify four main transitions centered at 336 K (0 Transition), 356 K (I Transition), 365 K (II Transition), and 373 K (III Transition).

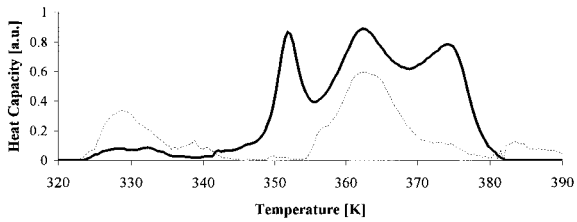

Fig. 2. Effects of nuclease digestion on logarithmic forms of *T. cruzi*. Thermal denaturation profiles of nuclei isolated from *T. cruzi* cells in logarithmic-phase growth before and after DNase I digestion. We can see the thermogram of logarithmic form of parasite in native conditions (dark line) versus the thermogram of logarithmic nuclei digested with DNase I (dashed line).

Figure 1 reports the calorimetric profile of nuclei isolated from rat hepatocytes: we can identify four main transitions centered at about 336 K (0 Transition), 356 K (I Transition), 365 K (II Transition), and 373 K (III Transition). Previous studies [Nicolini et al., 1983, 1988; Touchette and Cole, 1985; Barboro et al., 1993; Russo et al., 1995] supplied the correct assignment for all these peaks: the first broad peak (Transition 0) has been assigned to melting of nuclear proteins, Transition I to nucleosome organized in the unfolded nucleosomal filament of 10 nm, Transitions II and III to nucleosome organized in higher-order structures (fibers of 30 nm or more). After a gaussian decomposition, we can appreciate that Transition II is constituted by two components centered at 355 and 358 K (Transitions II_a and II_b) that represent the melting of linker and core DNA, respectively. Also, Transition III is constituted by two components centered at 371 and 375 K (Transitions III_a and III_b), which can be assigned to partially and highly folded chromatin [Allera et al., 1997; Vergani et al., 1998].

When we compare this thermogram with the one recorded on logarithmic growing parasites (Fig. 2a), we observe both similarities and differences: three main transitions are immediately evident in the usual temperature range, but their relative heights are significantly modified. For a quantitative analysis, we performed a gaussian deconvolution of the calorigram, and we observed that the melting temperatures are similar to the ones above reported for rat hepatocytes: Transition 0 at 330 K, Transition I at 349 K, Transition II at 362 K, and Transition III at 372 K. This result suggests a similarity in chromatin organization between *T. cruzi* and higher eukaryotic. However, *T. cruzi* chromatin profile is characterized by a slight shift of each transition towards lower temperatures. Taking into account that no previous works document a chromatin analysis performed on *T. cruzi* by means of DSC, we thought it necessary for a further control, to be sure of correctly assigning each peak. For instance, we analyzed nuclei isolated from log-phase parasites digested by DNase I, which introduces single-strand cuts inside the DNA double helix. When DNA is organized in the nucleosomal particle, DNase I cuts the linker-DNA, which is more accessible with respect to the core-DNA. So we should expect significant modifications of chromatin organization induced by an extensive digestion with this enzyme. In accordance with our expectations, and in analogy with previous results obtained on rat hepatocytes [Balbi et al., 1989], we observed a complete absence of Transition I and III, after DNase I digestion (Fig. 2b), with only a single broad peak at about 365 K remaining visible after the extensive digestion of DNA. Because we know that DNase I digestion induces a chromatin unfolding of the highly-condensed domains towards less compact structures [Touchette and Cole, 1985], we are now able to assign Transition I to the melting of linker-DNA and Transition II and III to melting of poly-nucleosomal chains organized in structures with different levels of condensation. Finally, the first broad peak (Transition 0), as for rat hepatocytes, is probably related to the denaturation of nuclear proteins.

In conclusion, the calorimetric analysis suggests that chromatin organization shows common aspects in different eukaryotic cells, without excluding significant differences between these organisms. First, in *T. cruzi*, with respect to rat hepatocytes, all the peaks are shifted towards lower temperatures, suggesting

a reduced stability of *T. cruzi* chromatin with respect to rat liver. This observation well fits with the observed lower stability of the parasite chromatin [Hecker and Gander, 1985]. Second, the single transitions show a redistribution of their melting enthalpies in comparison with rat hepatocytes: enthalpy of Transition II, in fact, becomes similar to those of Transition I and III (Table I). This means that *T. cruzi* chromatin exhibits in situ a different pattern of condensation in comparison with rat hepatocytes, even if the inner structure of the nucleosomal filament is similar, as suggested by the similarity of the melting temperatures.

Starting from these data, our attention was then focused on verifying the existence of significant modifications of chromatin organization in different forms of parasite. According to our expectations, we observed dramatic modifications of chromatin structure when we compare logarithmic growing parasites with stationary ones. Figure 3 shows that in stationary parasites, Transition III becomes prominent with respect to Transition II, while Transition I remains almost constant. These results suggest that when parasites enter into the stationary phase, the unfolded chromatin domains (Transition II) condense in more compact structures with higher melting temperatures (Transition III). Therefore, *T. cruzi* significantly remodels its nuclear chromatin during its phases of growth: a remarkable condensation of chromatin fibers it is associated with the stationary phase.

Analysis of Nuclear Architecture by Fluorescence Microscopy

The above data recorded significant structural differences between the two forms of parasite, at the level of chromatin condensation. It was then interesting to relate these differences with alterations of chromatin organization and nuclear architecture. To this aim, we employed high resolution fluorescence microscopy on whole cells of the two forms of *T. cruzi*. This approach has the advantage of introducing a minimum artifact, which, knowing the fragility of parasite chromatin [Astolfi et al., 1980; Hecker and Gander, 1985; Hecker et al., 1994], represents a relevant advantage in order to observe the native features of nuclear chromatin.

As previously reported [Belmont et al., 1989; Mascetti et al., 1996], the nuclear images acquired at high resolution (100 × magnification) can supply quantitative information about the organization and topographical distribution of chromatin domains inside a nucleus. Figure 4 reports the equatorial planes resulting from the image processing performed on two nuclei of parasites in different growing phases. Before the acquisitions, logarithmic and stationary cells of the parasite were properly stained with DAPI to selectively label the DNA. The distribution of the fluorescence inside the nucleus allowed us to extract the nuclear features characteristic of these two forms of the parasite. In both forms, we can see as the more condensed chromatin domains exhibit a characteristic triangle shape and are prevalently localized near to the nuclear envelope. In spite of these analogies, we observed a significant chromatin redistribution when parasites enter into stationary phase: the highly-folded chromatin domains become more defined and exhibit increased fluorescence intensity. Moreover, it is very interesting to observe as in logarithmic parasites the highly-compact domains seem to unfold towards the center of the nucleus. It has to be underlined that the electron microscopy micrographs suggested a similar behavior of the highly-condensed chromatin fibers. As reported in the same figure (Fig. 4), the well-defined electron-dense regions localize near the nuclear envelope in the stationary parasites, and they disappear in the logarithmic ones. Nuclear chromatin, therefore, suffers an

TABLE I. Relative Melting Enthalpy (Expressed in a.u.) Calculated for Each of the Four Main Thermal Transitions Observed in Nuclei Isolated From Rat Hepatocytes and Epimastigotes of *Trypanosoma cruzi

Nuclear sample	Transition 0 (330–336 K)	Transition I (349–357 K)	Transition II (360–365 K)	Transition III (371–373 K)
Rat hepatocytes	0.08 (336 K)	0.16 (356 K)	0.33 (365 K)	0.43 (373 K)
T. cruzi logarithmic phase	0.04 (330 K)	0.21 (349 K)	0.39 (362 K)	0.35 (372 K)
T. cruzi stationary phase	0.12 (333 K)	0.19 (349 K)	0.15 (360 K)	0.50 (371 K)

*Two different forms of the parasite were analyzed by DSC: logarithmic and stationary form, respectively. For each value, we also reported the exact melting temperature.

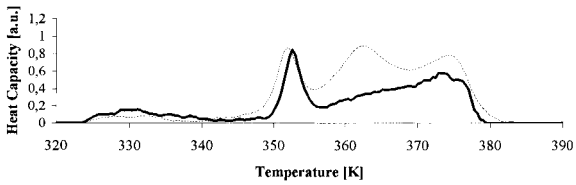

Fig. 3. Comparison between logarithmic and stationary forms of *T. cruzi*: DSC. The thermal denaturation profile of nuclei isolated from *T. cruzi* in stationary-phase growth is compared with the one acquired on logarithmic forms of the parasite. Thermogram of logarithmic forms of the parasite (dark line) and stationary one (dashed line).

average condensation when *T. cruzi* enters into a stationary growth phase; in fact a more homogeneous distribution of chromatin fibers is evident in nuclei of logarithmic growing parasites.

The images reported in Figure 4 are representative of the different cells analyzed for each form of the parasite. About 10 representative cells of each growing phase were elaborated and the intensitometric and morphometric parameters of each form of the parasite were calculated and reported in Table II. The previous works of our group [Nicolini et al., 1997; Mascetti et al., 2001; Vergani et al., 2001] demonstrated that in a native nucleus, the total DAPI uptake is inversely related to the average condensation of its chromatin. Therefore, if the DNA amount of a sample is constant, an increase of the integrated nuclear fluorescence Intensity is associated with an average unfolding of the chromatin fibers, while a reduction is associated with a condensation of the chromatin. We know that in logarithmic phase, parasites increase the amount of DNA: as previously documented [Sabaj et al., 1997] during the stationary phase of growth, both DNA and histone synthesis are extremely reduced, in comparison with the logarithmic phase. Anyway, the dramatic decrease of the integrated nuclear fluorescence intensity measured when parasites pass from logarithmic to stationary phase (from 8.9 to 3.3 a.u.) can be only partially due to the increased DNA content characteristic of log phase parasites. In fact, in log-phase the DNA content cannot exceed of more than twofold the stationary one. For this reason, the observed increase of fluorescence intensity can be partially ascribed to an increased DAPI uptake of logarithmic forms of the parasite, as a consequence of a less compact chromatin structure [Mascetti et al., 2001]. It is comforting that these observations are in accordance with the electron microscopy micrographs of isolated nuclei and with the calorimetric data, confirming that the stationary forms of *T. cruzi* present a more compact chromatin structure compared with the logarithmic one.

When we analyzed the nuclear morphometry, we can see the nucleus size is quite different

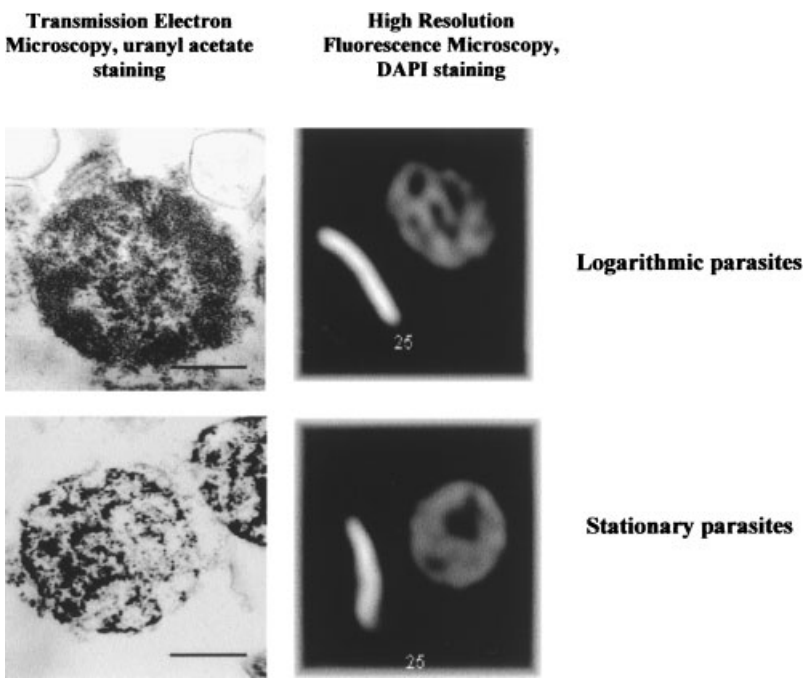

Fig. 4. Comparison between logarithmic and stationary forms of *T. cruzi*: fluorescence and electron microscopy. Equatorial plane of one representative nucleus acquired on native *T. cruzi* in two different forms: logarithmic and stationary. The images are acquired at high magnification (100 × objective) and mathematically processed in order to extract the inner nuclear features. Structural organization of chromatin within logarithmic and stationary nuclei analyzed by transmission electron microscopy, surprisingly shows the same distribution and compaction properties observed for intact cells.

TABLE II. Intensitometric and Morphometric Parameters Calculated on the Nuclear Images of *T. cruzi* Cells in Logarithmic and Stationary Phase*

Phase of cell growth	Length of nuclear major axis (μm)/SD	Length of nuclear minor axis 1 (μm)/SD	Nuclear area (μm^2)/SD	Integrated fluorescence intensity (a.u.)/SD	Intensity/area (a.u.)/SD
Logarithmic	1.80/0.24	1.37/0.16	1.92/0.46	$8.9E^{+06}/2.1E^{+06}$	$4.6E^{+06}/4.7E^{+06}$
Stationary	1.51/0.32	1.36/0.37	1.67/0.78	$3.3E^{+06}/1.9E^{+06}$	$2.0E^{+06}/2.4E^{+06}$

*For each sample, the images of about 5–10 cells were acquired and processed as described in Materials and Methods. For the optical sectioning, the nuclear images were acquired at different focal positions (0.1 μm intervals) along the z-axis in order to have from 64 to 128 slices within the sample.

between the two parasite forms (Table II). While the minor axis length is constant in both forms of *T. cruzi*, the major axis decreases by 0.3 μm when the parasite enters into the stationary form. This decrease of nuclear area in a two-dimensional space corresponds to a volume decrease in a three-dimensional space, under the condition that the nuclear thick is constant. The optical sectioning of nuclei of the two parasite forms made us able to estimate that the nuclear thick does not significantly change (Fig. 5). It is interesting to underline that the volume shrinking, which appears in the stationary parasite fits well with the average condensation observed for chromatin fibers in this phase of growth. In fact, an inverse relationship between nuclear volume and chromatin condensation was previously observed in other cellular systems [Vergani et al., 2001].

DISCUSSION

Chromatin in higher and lower eukaryotes is organized in classical nucleosome filaments, and also *T. cruzi*, as well as other ciliates (i.e., *Tetrehymena*, *Oxytricha*, *Paramecium*), shows this kind of organization [Hecker et al., 1994]. Also the biochemical properties of histones are similar in *T. cruzi* and higher eukaryotes [Toro and Galanti, 1990]. Despite of all these similarities, nevertheless, parasite chromatin shows a reduced capability of folding in highly compact structures, both in vivo (during mitosis) and also in vitro (in different ionic conditions). This characteristic behavior of *T. cruzi* chromatin was deduced when electron micrographs of rat liver chromatin were compared with those of *T. cruzi* under identical experimental conditions [Spadiliero et al., 2002].

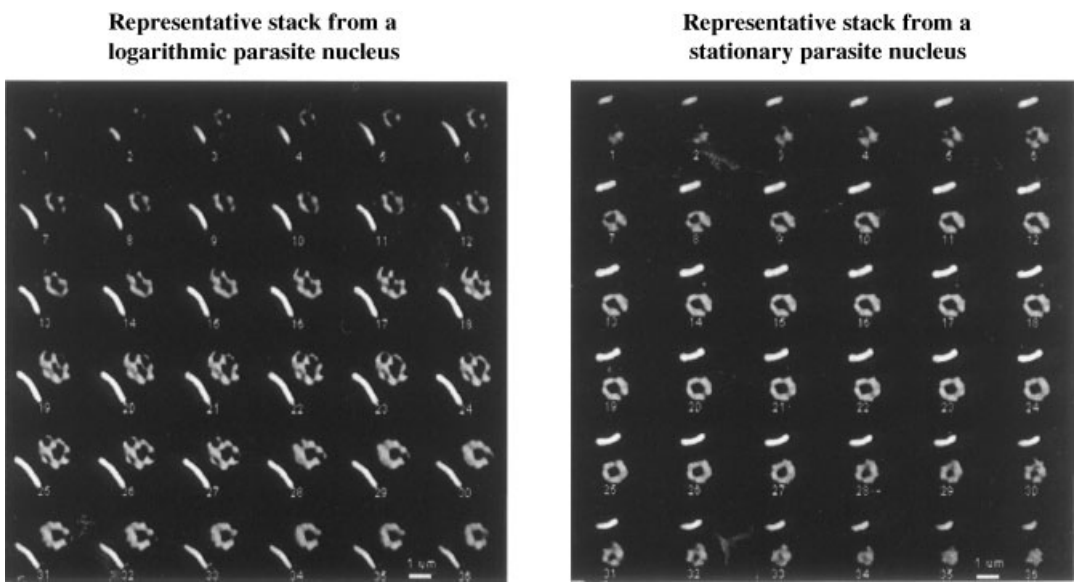

Fig. 5. Optical sectioning of *T. cruzi* nuclei: logarithmic versus stationary. The three-dimensional stacks of single nuclei have been acquired both for logarithmic (**a**) and stationary (**b**) forms of *T. cruzi*. Cells were stained with DAPI and images were mathematically processed as described in Materials and Methods.

An evident limit of this approach was essentially the invasivity of the electron microscopy technique, in particular for *T. cruzi* chromatin, which has an elevated instability [Hecker and Gander, 1985; Hecker et al., 1989]. For this reason, we thought it essential to analyze chromatin structure and organization of this parasite using non-invasive techniques, such as differential scanning calorimetry and fluorescence microscopy. Previous works [Nicolini et al., 1983; Balbi et al., 1988, 1989; Giartosio et al., 1992] demonstrated the structural organization of in situ chromatin can be successfully investigated by DSC technique, and a lot of studies were performed on different kinds of eukaryotic cells (i.e., thymocytes, hepatocytes, HeLa, CHO, etc.) in order to investigate the changes of chromatin structure associated with cell-cycle progression, differentiation, transformation, aging, etc.

We decided to follow the same biophysical approach for investigating chromatin organization in *T. cruzi*; we utilized as control the thermogram acquired on rat hepatocytes nuclei, which have been studied in details by DSC [Balbi et al., 1989; Nicolini et al., 1988]. Interesting conclusions can be drawn from DSC data. First of all, we confirm that *T. cruzi* chromatin is on average less condensed than in other higher eukaryotes (such as rat hepatocytes), as is suggested by the imbalance in the enthalpy of the thermal transitions associated to chromatin melting (Transition II and III). Second, the same three levels of condensation, typical of higher eukaryotes, appear also in *T. cruzi*: unfolded nucleosomal filaments, partially-folded chromatin fibers, and highly folded fibers. On this basis, we can conclude that nuclear chromatin of this parasite is organized similarly as well it occurs in other higher eukaryotes. Third, we confirmed that parasites suffer an average condensation of their chromatin fibers when they enter into the stationary growth phase.

Resuming the above observations, we can affirm that in a parasite there is a dynamic balance between the three levels of chromatin condensation (from the unfolded till to the highly folded one). This equilibrium is continuously modulated during the parasite growth, and it could be controlled by the folding/unfolding cell machinery, which is well characterized for higher eukaryotes, but not yet described for *T. cruzi*. We previously observed that at high salt concentrations soluble chromatin fibers isolated from stationary parasites condense more than the logarithmic ones. In parallel, a highly-folded organization in chromatin of stationary parasites was suggested by nuclease digestion experiments [Spadiliero et al., 2002].

The parallel analysis performed by fluorescence microscopy on intact cells demonstrated that the remodeling of chromatin folding observed by DSC during the parasite growth is accompanied by a significant redistribution of chromatin domains inside the nuclear volume. This is important because till now no mechanism of gene silencing/activation induced by chromatin remodeling was hypothized for *T. cruzi*. Only post-transcriptional mechanisms were in fact considered as possible events of gene expression control [Texeira, 1998; D'Orso and Frasch, 2001]. Our data on the contrary suggest that in *T. cruz*, we are in the presence of a dynamic chromatin structure, which could play a role in the activation/silencing of genes.

On the light of our observations, we propose a model to explain the mechanisms by which *T. cruzi* chromatin structure could regulate gene expression. For this hypothetical model, we started from the particularities exhibited by the parasite nucleus, in particular the preservation of the nuclear envelope during mitosis. In higher eukaryotes, the nuclear envelope (nuclear matrix plus lamina) is known to represent a scaffold for the entire nucleus; on the contrary, this function is not described for *T. cruzi*. Other important features of nuclear organization have been considered in our model. First, the flexibility of the nuclear envelope, which could allow the parasite to control the nuclear volume, depending on the folding status of chromatin. Second, the chromatin distribution within the nucleus, which is not random. In fact, the chromatin domains localized near the nuclear envelope are persistent during the different phases of parasite growth. Third, the process of chromatin unfolding that we observed in logarithmic cells, seems to proceed from the periphery toward the center of the nucleus by apparently using the nuclear envelope as attachment site.

Based on these data, we suppose that this ancient parasite chooses a very simple mechanism to regulate its minimal requirements of chromatin remodeling. Our model reported in Figure 6 tries to correlate structural with

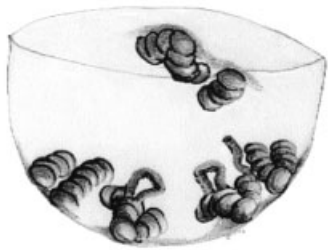

Idealized representation of chromatin fibers distribution within a stationary hemisected nucleus

Idealized representation of chromatin fibers distribution within a logarithmic hemisected nucleus

Fig. 6. Schematic model of nuclear organization in *T. cruzi* cells. Models of nuclear architecture, which try to explain the modulation of chromatin structure during the growth curve of parasite. The stationary form presents a smaller nucleus, with chromatin more condensed and localized near to the nuclear envelope forming triangle-shaped regions. Logarithmic form preserves the folded domains near the membrane, but shows an increased nuclear diameter and a less condensed chromatin more homogenously distributed inside the nucleus. The folding/unfolding of chromatin of *T. cruzi* could occur from the nuclear membrane toward the central region of nucleus.

functional observations. Maintaining an anchorage system, represented by the nuclear envelope, the process of chromatin folding/unfolding could take place from the periphery towards the central region of the nucleus, when the parasite is in a logarithmic phase of growth (where a more relaxed chromatin structure is required). On the contrary, during the stationary phase, a reverse process guarantees the folding of chromatin fibers into more compact domains, which present attachment sites near to the nuclear envelope.

OUTLOOK

The prosecution of this work will require a deeper structural and biochemical characterization of the transcriptionally active chromatin of *T. cruzi*. The DNA of transcribing genes can be purified from parasite chromatin and by a Southern blot, and we can reveal the level of transcription of genes associated with a specific state of chromatin folding. In parallel, the post-translational modifications of parasite histones (acetylation and phosphorylation, mainly) can be analyzed depending on the specific phase of parasite life cycle.

ACKNOWLEDGMENTS

Our special gratitude to Prof. Eugenio Debbia, Director of the Institute of Microbiology at San Martino Hospital of Genova, who provided proper safety areas for the cell culture of *T. cruzi*. We also wish to extend our gratitude to Cristina Rando and Fabrizio Nozza for their technical assistance. Dr. Spadiliero was sponsored by a fellowship financed by Ambasciata Italiana in Caracas (Venezuela) and Ministry for Foreign Affairs of Italy.

REFERENCES

Astolfi Fihlo S, Martins de Sá C, Gander S. 1980. On the chromatin structure of *Trypanosoma cruzi*. Mol Biochem Parasitol 1:45–53.

Allera C, Lazzarini G, Patrone E, Alberti I, Barboro P, Sanna P, Melchiori A, Parodi S, Balbi C. 1997 The condensation of chromatin in apoptotic thymocytes shows a specific structural change. J Biol Chem 272(16):10817–10822.

Balbi C, Abelmoschi ML, Zunino A, Cuniberti C, Cavazza B, Barboro P, Patrone E. 1988. The decondensation process of nuclear chromatin as investigated by differential scanning calorimetry. Biochem Pharmacol 37:1815–1816.

Balbi C, Abelmoschi ML, Gogioso L, Parodi S, Barboro P, Cavazza B, Patrone E. 1989. Structural domains and conformational changes in nuclear chromatin: a quantitative thermodynamic approach by differential scanning calorimetry. Biochemistry 28:3220–3227.

Barboro P, Pasini A, Parodi S, Balbi C, Cavazza B, Allera C, Lazzarini G, Patrone E. 1993. Chromatin changes in cell transformation: a differential scanning calorimetry study. Biophys J 65:1690–1699.

Belli SI. 2000. Chromatin remodeling during the life cycle of trypanosomatids. Int J Parasitol 30:679–687.

Belmont AS, Braunfeld MB, Sedat JW, Agard DA. 1989. Large-scale chromatin structural domains within mitotic and interphase chromosomes in vivo and in vitro. Chromosoma 98:129–143.

Burgoyne LA, Waqar NA, Atkinson NR. 1970. Calcium-dependent priming of DNA synthesis in isolated rat liver nuclei. Biochem Biophys Res Comm 39(2):254–259.

D'Orso I, Frasch AC. 2001. TcUBP-1, a developmentally regulated U-rich RNA-binding protein involved in selective mRNA destabilization in trypanosomes. J Biol Chem 276(37):34801–34809.

Gavazzo P, Vergani L, Mascetti G, Nicolini C. 1997. Effects of histone acetylation on higher order chromatin structure and function. J Cell Biochem 64(3):466–475.

Giartosio A, Wang C, D'Alessio S, Ferraro A, Altieri F, Eufemi M, Turano C. 1992. Differential scanning calorimetry of chicken erythrocyte nuclei. FEBS 200:17–22.

Hecker H, Gander ES. 1985. The compactation pattern of the chromatin of trypanosomes. Biol Cell 53:199–208.

Hecker H, Bender K, Betschart B, Modespacher U-P. 1989. Instability of the nuclear chromatin of procyclic *Trypanosoma brucei brucei*. Mol Biochem Parasitol 37:225–234.

Hecker H, Betschart B, Bender K, Burri M, Schlimme W. 1994. The chromatin of trypanosomes. Int J Parasitol 24(6):809–819.

Herwaldt BL. 1999. Leishmaniasis. Lancet 359:1191–1199.

Hiraoka Y, Sedat JW, Agard DA. 1987. The use of a charge-coupled device for quantitative optical microscopy of biological structures. Science 238:36–41.

Kurz A, Lampel S, Nikolenko JE, Bradl J, Benner A, Zirbel RM, Cremer T, Lichter P. 1996. Active and inactive genes localize preferentially in the periphery of chromosome territories. J Cell Biol 135(5):1195–1205.

Mascetti G, Vergani L, Diaspro A, Carrara S, Radicchi G, Nicolini C. 1996. Effect of fixatives on calf thymocytes chromatin as analyzed by 3D high-resolution fluorescence microscopy. Cytometry 23:110–125.

Mascetti G, Carrara S, Vergani L. 2001. The relationship between fiber folding and dye uptake for in situ chromatin stained with a DNA-selective dye. Cytometry 44(2):113–119.

Myc A, Traganos F, Lara J, Melamed MR, Darzynkiewicz Z. 1992. DNA stainability in aneupolodia breast cancer tumors: comparison of four DNA fluorochromes differing in binding properties. Cytometry 13:389–394.

Nicolini C, Trefiletti V, Cavazza B, Cuniberti C, Patrone E, Carlo P, Brambilla G. 1983. Quaternary and quinternary structure of chromatin from resting cells: high resolution computer analysis of liver nuclei and differential scanning calorimetry. Science 219(4581):176–178.

Nicolini C, Diaspro A, Vergani L, Cittadini G. 1988. In situ thermodynamic characterization of chromatin and of other cell macromolecules during cell cycle. Int J Biol Macromol 10:137–144.

Nicolini C, Carrara S, Mascetti G. 1997. High order DNA structure inferred by optical fluorimetry and scanning calorimetry. Mol Biol Rep 24:235–246.

Reynolds ES. 1963. The use of lead citrate at high pH as an electron opaque stain in electron microscopy. J Cell Biol 17:208–211.

Rubio J, Rosado Y, Castaneda M. 1980. Subunit structure of *Trypanosoma cruzi* chromatin. Can J Biochem 58: 1247–1251.

Russo I, Barboro P, Alberti I, Parodi S, Balbi C, Allera C, Lazzarini G, Patrone E. 1995. Role of H1 in chromatin folding: a thermodynamic study of chromatin reconstitution by DSC. Biochemistry 34:301–311.

Sabaj V, Díaz J, Toro GC, Galanti N. 1997. Histone synthesis in *Trypanosoma cruzi*. Exp Cell Res 236:446–452.

Schlimme W, Burri M, Bender K, Betschart B, Hecker H. 1993. *Trypanosoma brucei brucei*: differences in the nuclear chromatin of bloodstream forms and procyclic culture forms. Parasitology 107:237–247.

Schmidt GT, Roberts LS. 1989. Foundations of Parasitology. Times Mirror/Mosby College Publishing New York, USA. 4th Edition, pp. 83–98.

Spadiliero B, Sánchez F, Slezynger T, Henríquez D. 2002. Differences in the nuclear chromatin among various stages of the life cycle *Trypanosoma cruzi*. J Cell Biochem 84:832–839.

Texeira SM. 1998. Control of gene expression in Trypanosoma cruzi. Braz J Med Biol Res 31(12):1503–1516.

Toro C, Galanti N. 1990. *Trypanosoma cruzi* histones. Further characterization and comparison with higher eukaryotes. Biochem Int 21:481–490.

Toro CG, Galanti N, Hellman U, Wernstedt C. 1993. Unambiguous identification of histone H1 in *Trypanosoma cruzi*. J Cell Biochem 52:431–439.

Touchette NA, Cole RD. 1985. Differential scanning calorimetry of nuclei reveals the loss of major structural features in chromatin by brief nuclease treatment. Proc Nat Acad Sci USA 82:2642–2645.

Vergani L, Gavazzo P, Facci P, Diaspro A, Mascetti G, Arena N, Gaspa L, Nicolini C. 1992. Fluorescence cytometry of microtubules and nuclear DNA during cell-cycle and reverse transformation. J Cell Biochem 50:201–209.

Vergani L, Mascetti G, Nicolini C. 1998. Effects of polyamines on higher-order folding on in situ chromatin. Mol Biol Rep 25(4):237–244.

Vergani L, Fugazza G, Chessa L, Nicolini C. 1999. Changes of chromatin condensation in one patient with Ataxia Telangiectasia disorder: A structural study. J Cell Biochem 75:578–586.

Vergani L, Mascetti G, Nicolini C. 2001. Changes of nuclear structure in used by increasing temperature. J Biomol Struct Dyn 18(4):535–544.

Wolffe AP, Hayes JJ. 1999. Chromatin disruption and modification. Nucleic Acid Res 27:711–720.

Wolffe AP, Matzke A. 1999. Epigenetics: regulation through repression. Science 286:481–486.

Zinc D, Cremer T, Saffrich R, Fischer R, Trendelenburg MF, Ansorge W, Stelzer EHK. 1998. Structure and dynamics of human interphase chromosomes territories in vivo. Hum Genet 102:241–251.